AIMS Mathematics, 10(8): 17543–17566.
DOI:10.3934/math.2025784
Received: 24 April 2025
Revised: 13 July 2025
Accepted: 18 July 2025
Published: 01 August 2025

https://www.aimspress.com/journal/Math

Research article

Propagation of nonlinear dispersive waves in shallow water and acoustic media in the framework of integrable Schwarz–Korteweg–de Vries equation

Khizar Farooq[1], **Ejaz Hussain**[2], **Hamza Ali Abujabal**[3] **and Fehaid Salem Alshammari**[4,*]

[1] Centre for High Energy Physics, University of the Punjab, Quaid-e-Azam Campus, Lahore 54590, Pakistan

[2] Department of Mathematics, University of the Punjab, Quaid-e-Azam Campus, Lahore 54590, Pakistan

[3] Department of Mathematics, Faculty of Science, King Abdulaziz University, P. O. Box 80003, Jeddah 21589, Saudi Arabia

[4] Department of Mathematics and Statistics, College of Science, Imam Mohammad Ibn Saud Islamic University (IMSIU), Riyadh, Saudi Arabia

* **Correspondence:** Email: falshammari@imamu.edu.sa.

Abstract: This article investigated the solitary wave solutions to the (2+1)-dimensional integrable Schwarz–Korteweg–de Vries equation. The proposed model is particularly applicable to shallow water wave dynamics and may also extend to contexts such as acoustic wave propagation, nonlinear electric media, and oceanic wave phenomena. First, we constructed the ordinary differential equation form of the nonlinear partial differential equation with the help of the traveling wave transformation. After that, we utilized the generalized Arnous method and the modified sub-equation method to construct the solitary waves containing hyperbolic, exponential, trigonometric, and inverse functions. Using suitable parameter values, the graphical aspects of solutions are demonstrated by plotting a 3D surface plot (including a contour and density plot), a 2D surface plot, a streamline plot, and a polar plot. By utilizing these approaches, accurate analytical solutions for soliton waves were generated, which comprise kink, bright, and dark waves. We employed the generalized Arnous method and the modified sub-equation method to formulate a technique for addressing integrable systems, providing a valuable framework for examining nonlinear phenomena across various physical contexts. This study's outcomes enhance both nonlinear dynamical processes and solitary wave theory.

Keywords: (2+1)-dimensional integrable Schwarz–Korteweg–de Vries equation; generalized Arnous method; modified sub-equation method
Mathematics Subject Classification: 26A48, 26A51, 33B10, 37K40, 39B62

1. Introduction

In recent years, scientists have recognized the complexity and subtlety of natural patterns, which require a more complete understanding. Exploring these nuanced phenomena demands advanced tools and methods, such as partial differential equations (PDEs) that can be used to describe these phenomena by modeling them. Additionally, 3D imaging techniques have been developed to gain insight into these processes. PDEs are used to model intricate patterns and behaviors, forming the foundation for understanding physical systems, and their coordinated dynamics.

A soliton is a unique type of wave that can travel across a distance without changing its shape or losing energy even after interacting with other waves. Unlike broad-spectrum, conventional waves, solitons exhibit extreme stability and persistence. These qualities make them critical to various research areas such as nonlinear optics [1], plasma physics [2], hydrodynamics [3], biology [4], engineering [5], mechanics [6], communication systems [7], optical fibers [8], and fluid dynamics [9, 10]. Solitons offer critical insights and significantly contribute to advancements across these fields. Analyzing solitary wave solutions of nonlinear partial differential equations (NLPDEs) is essential for a deeper understanding of the physical processes they represent. From a practical perspective, NLPDEs are particularly important, because they offer a more detailed and nuanced description of physical, chemical, and biological processes. Solitary wave solutions of NLPDEs are especially noteworthy, and can be studied and solved using many different techniques, including the extended auxiliary equation mapping method [11], Backlund transform method [12], exp-function method [13], improved extended fan-sub equation method [14], homotopy perturbation method [15], generalized Kudryashov method [16], Hirota bilinear method [17], extended trial equation method [18], Darboux transformation [19], modified extended tanh method, extended simple equation method [20], novel $(\frac{G'}{G})$ expansion method [21], extended direct algebraic method [22], exp $(-\chi(\Theta))$ expansion method [23], and extended mapping method [24], among others [25, 26]. These approaches have greatly contributed to advancing the understanding and solving of NLPDEs. Alongside solitary wave solutions, chaotic behavior, bifurcation analysis [27], and sensitivity analysis [28] play an essential part in characterizing the fundamental behavior of NLPDEs.

NLPDEs have emerged as important tools in scientific research, offering useful insights into fields such as plasma, dynamics, acoustics, optics, and condensed matter physics. These equations not only deepen our understanding of complex phenomena but also enable precise predictions of their future development. Consequently, researchers continue to investigate a wide variety of NLPDEs to better understand complex behaviors in natural systems. Recent studies have examined equations such as the Schrödinger equation [29, 30], Batman-Burger equation [31], Benjamin-Bona-Mahony equation [32], Date-Jimbo-Kashiwara-Miwa equation [33], thin-film ferroelectric material equation [34], Boussinesq equation [35], Buckmaster equation [36], and nonlinear non-classical Sobolev-type wave model [37], nonlinear Boiti-Leon-Manna-Pempinelli model [38], among many others [39, 40].

Joseph Boussinesq first proposed the Korteweg-de Vries (KdV) equation in 1877, which was then refined and disseminated by Diederik Korteweg and Gustav de Vries in 1895. This equation is a fundamental model in fluid dynamics. It is renowned for describing the propagation of nonlinear dispersive waves in shallow water. The standard form of the KdV equation is [41]:

$$\mathcal{P}_t + \mathcal{W}_{xxx} - 6\,\mathcal{W}\,\mathcal{W}_{xxx} = 0. \tag{1.1}$$

In the context of weakly nonlinear shallow water waves, U(x, t) characterizes the wave profile as a function of spatial coordinates x and t. The KdV equation has been adapted and extended into various forms to address more complex physical scenarios. One notable extension is the Schwarz-Koeteweg-de Vries (SKdV) equation, whose form is as follows:

$$\mathcal{P}_t + \mathcal{P}_x\left[\left(\frac{\mathcal{P}_{xx}}{\mathcal{P}_x}\right) - \frac{1}{2}\left(\frac{\mathcal{P}_{xx}}{\mathcal{P}_x}\right)^2\right] = 0. \tag{1.2}$$

Here $\mathcal{P}(x, t)$ denotes the unknown wave function that was originally derived by Krichever, Noviko [42], and Wesis [43, 44] to account for higher-order effects and extend the scope of the classical KdV equation.

In this work, we investigate the (2+1)-dimensional integrable Schwarz–Korteweg–de Vries equation (ISKdV), which incorporates an additional spatial dimension for modeling more complex wave dynamics. The generalized equation is expressed as:

$$\mathcal{W} + \frac{1}{4}\mathcal{W}_{xxy} - \frac{\mathcal{W}_x\mathcal{W}_{xy}}{2\mathcal{W}} - \frac{\mathcal{W}_{xx}\mathcal{W}_y}{4\mathcal{W}} + \frac{\mathcal{W}_x^2\mathcal{W}_y}{2\mathcal{W}^2} - \frac{\mathcal{W}_x}{8}\int\left(\frac{\mathcal{W}_x^2}{\mathcal{W}^2}\right)_y dx = 0. \tag{1.3}$$

Toda and Yu [45] derived Eq (1.3). By applying the following transformation on Eq (1.3),

$$\mathcal{W} = \mathcal{T}_x, \quad \mathcal{T} = e^{\mathcal{H}}, \quad \mathcal{H}_x = \mathcal{W}, \quad \mathcal{H}_t = \mathfrak{P}. \tag{1.4}$$

Here, $\mathcal{T}(x,t)$,$\mathcal{H}(x,t)$,$\mathcal{T}(x,t)$,$\mathcal{W}(x,t)$, $\mathfrak{P}(x,t)$ represent the unknown functions, and we derive the following results:

$$\begin{cases} 4\mathcal{W}^2\mathfrak{P}_x - 4\mathcal{W}\mathcal{W}_x\mathfrak{P} + \mathcal{W}^2\mathcal{W}_{xxy} - \mathcal{W}\mathcal{W}_{xx}\mathcal{W}_y - 3\mathcal{W}\mathcal{W}_x\mathcal{W}_{xy} + 3\mathcal{W}_x^2\mathcal{W}_y - \mathcal{W}_x^4\mathcal{W}_y = 0, \\ \mathcal{W}_t - \mathfrak{P}_x = 0. \end{cases} \tag{1.5}$$

The equation presented originates from the research by Bruzon [46]. By applying the Miura transformation [47, 48] to Eq (1.5), the following expression can be derived:

$$\begin{cases} \mathfrak{R}_x = \frac{\mathcal{W}_{xx}}{4\mathcal{W}} - \frac{\mathcal{W}_x^2}{8\mathcal{W}^2} - \frac{\mathcal{W}^2}{8}, \\ \mathfrak{R}_y = \frac{\mathfrak{P}}{\mathcal{W}}. \end{cases} \tag{1.6}$$

and we obtain [49]

$$4\mathfrak{R}_{xt} + 8\mathfrak{R}_{xy}\mathfrak{R}_x + 4\mathfrak{R}_{xt} + \mathfrak{R}_{xxxy} + 8\mathfrak{R}_{xy}\mathfrak{R}_x + 4\mathfrak{R}_y\mathfrak{R}_{xx} = 0. \tag{1.7}$$

The ISKdV model has been widely investigated by several researchers. Khater investigated a novel solitary solution for the ISKdV model utilizing the Khater methodology and Bernoulli sub-equation approach [50]. Attia et al. focused on numerical and computational solutions for the same model using the Miura transform [51]. Prior to investigating various soliton excitations of the ISKdV model, Li et al. employed the Darboux transformation [52] to derive soliton solutions [53]. Ramirez et al. applied the Mobius transformation to examine different solutions for the ISKdV model [46]. Toda et al. studied soliton solutions using Lax pairings and a higher-dimensional method [54].

Gandarias et al. conducted classical symmetry reductions of the ISKdV model by applying symmetries and arbitrary functions [55]. Lastly, Aslan investigate solutions of the ISKdV model using an enhanced technique [56].

After a complete assessment of the available literature, we found no publications addressing the ISKdV model through the generalized Arnous approach and modified sub-equation method. As such, here we provide the generalized solutions to the ISKdV model using the generalized Arnous approach and the modified sub-equation method. These findings not only highlight the multitude of ways utilized to analyze Eq (1.7) but also emphasize the significance of studying multiple solution strategies for a full knowledge of its dynamics.

This paper is structured as follows: In Section 2, the given PDE is converted into an ODE by applying traveling wave transformation. In Section 3, we apply the generalized Arnous method to construct solitary waves. Section 4 presents the accurate derivations of solutions of Eq (1.7) via the modified sub-equation method. Finally, Section 6 summarizes the paper.

2. Mathematical investigation

The generalized NLPDE can be expressed in the following form:

$$\mathfrak{L}(\mathfrak{R}, \mathfrak{R}_t, \mathfrak{R}_x, \mathfrak{R}_y, \mathfrak{R}_z, \mathfrak{R}_{t,t}, \mathfrak{R}_{x,x}, ...) = 0. \tag{2.1}$$

While the function $\mathfrak{R} = \mathfrak{R}(t, y, x)$ is still not known, by applying the below transformation, we can convert the NPLDE as shown in Eq (1.7) into an ODE.

$$\mathfrak{R}(t, y, x) = \mathfrak{F}(\xi), \quad \xi = \delta x + \mu y + \omega t. \tag{2.2}$$

As a result, the ODE has the following form:

$$\mathfrak{T}(\mathfrak{F}, \mathfrak{F}', \mathfrak{F}'', \mathfrak{F}''', ...) = 0. \tag{2.3}$$

To obtain the exact solution of Eq (1.7), it is assumed that the equation allows traveling wave transformation. The assumption arises from the compatibility of the transformation outline in Eq (2.2) with Eq (1.7). With Eq (2.2) substituted in Eq (1.7), it reduces to the following ODE:

$$4\omega\mathfrak{F}' + \delta^2\mu\mathfrak{F}''' + 6\delta\mu\mathfrak{F}'^2 = 0. \tag{2.4}$$

If we let $\mathfrak{F}' = \mathfrak{S}$, Eq (2.4) becomes:

$$4\omega\mathfrak{S} + \delta^2\mu\mathfrak{S}'' + 6\delta\mu\mathfrak{S}^2 = 0. \tag{2.5}$$

3. The generalized Arnous method

The basic steps of the generalized Arnous (GA) method are as follows:
Step 01: The GA method provides the solution of Eq (2.4) as follows:

$$\mathfrak{F}(\xi) = y_0 + \sum_{1=1}^{N} \frac{y_i + z_i\,(\mathfrak{p}'(\xi))^i}{\mathfrak{p}(\xi)^i}. \tag{3.1}$$

where y_i, z_i (for i = 1, 2, . . . , N), $\frac{1}{\mathfrak{p}(\xi)^i}$, which is valid for when $\mathfrak{p}(\xi) \neq 0$ are constants with constraint $y_N^2 + z_N^2 \neq 0$, and the function $\mathfrak{p}(\xi)$ verifies the relation

$$[\mathfrak{p}'(\xi)]^2 = [\mathfrak{p}(\xi)^2 - \epsilon] \ln[F]. \tag{3.2}$$

with,

$$\mathfrak{p}^{(n)}(\xi) = \begin{cases} \mathfrak{p}(\xi) \ln(F)^n, & \text{if } n \text{ is even,} \\ \mathfrak{p}'(\xi) \ln(F)^{n-1}, & \text{if } n \text{ is odd,} \end{cases} \tag{3.3}$$

where $n \geq 2$, and $0 < F \neq 1$, and $\ln F$ is defined for a positive real number. Then, Eq (3.2) has solutions of the following form:

$$\mathfrak{p}(\xi) = \beta \ln(F) F^{\xi} + \frac{\epsilon}{4\beta \ln(F) F^{\xi}}. \tag{3.4}$$

where β, F, and ϵ are arbitrary real parameters, but Eq (3.4) will become undefined when $\beta = 0, \ln F = 0$, and F=1.

Step 02: By balancing the nonlinear term and the term with the highest order derivative in Eq (2.5), the positive integer N is determined for Eq (3.1).

Step 03: After inserting Eqs (3.2) and (4.20) in Eq (2.5), and since $\mathfrak{p}^i(\xi) \neq 0$, as a result of this substitution, we get a polynomial of $\frac{1}{\mathfrak{p}(\xi)}\left(\frac{\mathfrak{p}'(\xi)}{\mathfrak{p}(\xi)}\right)$. Equivalently, we set all terms with the same power to zero. Then, by solving this set of non-linear algebraic systems and with the help of Eqs (4.17) and (2.2), the solutions of Eq (1.7) may be determined.

3.1. Solitary wave solution by generalized Arnous method

To find the exact solution of Eq (2.5), first we find the value of the positive integer $N = 2$. Adding the value of N to Eq (3.1), then Eq (3.1) will become as follows:

$$\mathfrak{F}(\xi) = x_0 + \frac{y_1}{\mathfrak{p}(\xi)} + \frac{z_1 \mathfrak{p}'(\xi)}{\mathfrak{p}(\xi)} + \frac{y_2}{\mathfrak{p}(\xi)^2} + \frac{z_2(\mathfrak{p}''(\xi))^2}{\mathfrak{p}(\xi)^2}. \tag{3.5}$$

By inserting Eq (3.5) into Eq (2.4), together with Eq (2.4) and Eq (3.2), we have a polynomial in terms of $\frac{1}{\mathfrak{p}(\xi)}\left(\frac{\mathfrak{p}'(\xi)}{\mathfrak{p}(\xi)}\right)$. This creates a system of algebraic equations when we aggregate all terms of the same power and equal them to zero. The values of unknown constants are obtained.

Set 1.

$$y_1 = 0, \quad z_1 = 0, \quad y_2 = \epsilon \ln^2(F) z_2. \tag{3.6}$$

By putting set 1 in Eq (3.5), we obtain the exact solution as follows:

$$\mathfrak{R}_1(t, x, y) = \frac{z_2 \epsilon \ln^2(F)}{\left(\frac{\epsilon F^{-\xi}}{4\beta \ln(F)} + \beta F^{\xi} \ln(F)\right)^2} + \frac{z_2 \left(\beta F^{\xi} \ln^2(F) - \frac{\epsilon F^{-\xi}}{4\beta}\right)^2}{\left(\frac{\epsilon F^{-\xi}}{4\beta \ln(F)} + \beta F^{\xi} \ln(F)\right)^2} + x_0. \tag{3.7}$$

when we choose F = e and $\epsilon = 4\beta^2$, the Eq (3.7) will be

$$\mathfrak{R}_2(t, x, y) = z_2 \tanh^2(t\omega + \delta x + \mu y) + z_2 \mathrm{sech}^2(t\omega + \delta x + \mu y) + x_0. \tag{3.8}$$

when we choose F = e and $\epsilon = -4\beta^2$, the Eq (3.7) will be

$$\Re_3(t,x,y) = z_2 \coth^2(t\omega + \delta x + \mu y) - z_2 \mathrm{csch}^2(t\omega + \delta x + \mu y) + x_0. \tag{3.9}$$

Set 2.

$$y_1 = 0, z_1 = 0, y_2 = \frac{\epsilon z_2}{\delta^2}, F = \frac{1}{\delta}, \mu = -\frac{4\omega}{\delta^2 \ln^2(\delta)}. \tag{3.10}$$

By putting set 2 in Eq (3.5), we obtain the exact solution as follows:

$$\begin{aligned}\Re_4(t,x,y) = y_0 + \frac{\epsilon z_2}{\delta^2\left(\frac{\left(\frac{1}{\delta}\right)^{-x\delta - t\omega + \frac{4y\omega}{\delta^2\ln^2(\delta)}}\epsilon}{4\beta\ln\left(\frac{1}{\delta}\right)} + \beta\left(\frac{1}{\delta}\right)^{x\delta + t\omega - \frac{4y\omega}{\delta^2\ln^2(\delta)}}\ln\left(\frac{1}{\delta}\right)\right)^2} + \\ \frac{\left(-\frac{\left(\frac{1}{\delta}\right)^{-x\delta - t\omega + \frac{4y\omega}{\delta^2\ln^2(\delta)}}\epsilon}{4\beta} + \beta\left(\frac{1}{\delta}\right)^{x\delta + t\omega - \frac{4y\omega}{\delta^2\ln^2(\delta)}}\ln\left(\frac{1}{\delta}\right)^2\right)^2 z_2}{\left(\frac{\left(\frac{1}{\delta}\right)^{-x\delta - t\omega + \frac{4y\omega}{\delta^2\ln^2(\delta)}}\epsilon}{4\beta\ln\left(\frac{1}{\delta}\right)} + \beta\left(\frac{1}{\delta}\right)^{x\delta + t\omega - \frac{4y\omega}{\delta^2\ln^2(\delta)}}\ln\left(\frac{1}{\delta}\right)\right)^2}).\end{aligned} \tag{3.11}$$

when we choose F = e and $\epsilon = 4\beta^2$, the Eq (3.11) becomes

$$\Re_5(t,x,y) = y_0 + \frac{\ln^2\left(\frac{1}{\delta}\right)\left(\left(\frac{1}{\delta}\right)^{-2+\frac{16y\omega}{\delta^2\ln^2(\delta)}} + \left(\frac{1}{\delta}\right)^{-2+4x\delta+4t\omega}\ln\left(\frac{1}{\delta}\right)^4 - 2\left(\frac{1}{\delta}\right)^{2x\delta+2t\omega+\frac{8y\omega}{\delta^2\ln^2(\delta)}}\left(-2+\delta^2\ln^2\left(\frac{1}{\delta}\right)\right)\right)z_2}{\delta^2\left(\left(\frac{1}{\delta}\right)^{\frac{8y\omega}{\delta^2\ln^2(\delta)}} + \left(\frac{1}{\delta}\right)^{2(x\delta+t\omega)}\ln^2\left(\frac{1}{\delta}\right)\right)^2}. \tag{3.12}$$

when we choose F = e and $\epsilon = -4\beta^2$, the Eq (3.11) becomes

$$\Re_6(t,x,y) = y_0 + \frac{\ln^2\left(\frac{1}{\delta}\right)\left(\left(\frac{1}{\delta}\right)^{-2+\frac{16y\omega}{\delta^2\ln^2(\delta)}} + \left(\frac{1}{\delta}\right)^{-2+4x\delta+4t\omega}\ln\left(\frac{1}{\delta}\right)^4 + 2\left(\frac{1}{\delta}\right)^{2x\delta+2t\omega+\frac{8y\omega}{\delta^2\ln^2(\delta)}}\left(-2+\delta^2\ln^2\left(\frac{1}{\delta}\right)\right)\right)z_2}{\delta^2\left(\left(\frac{1}{\delta}\right)^{\frac{8y\omega}{\delta^2\ln^2(\delta)}} - \left(\frac{1}{\delta}\right)^{2(x\delta+t\omega)}\ln^2\left(\frac{1}{\delta}\right)\right)^2}. \tag{3.13}$$

Set 3.

$$y_1 = 0, z_1 = 0, y_2 = \delta^2\epsilon z_2, F = \delta. \tag{3.14}$$

By putting set 3 in Eq (3.5), we obtain the exact solution as follows:

$$\Re_7(t,x,y) = y_0 + \frac{\delta^2\epsilon z_2}{\left(\frac{\delta^{-x\delta-y\mu-t\omega}\epsilon}{4\beta\ln(\delta)} + \beta\delta^{x\delta+y\mu+t\omega}\ln(\delta)\right)^2} + \frac{\left(-\frac{\delta^{-x\delta-y\mu-t\omega}\epsilon}{4\beta} + \beta\delta^{x\delta+y\mu+t\omega}\ln(\delta)^2\right)^2 z_2}{\left(\frac{\delta^{-x\delta-y\mu-t\omega}\epsilon}{4\beta\ln(\delta)} + \beta\delta^{x\delta+y\mu+t\omega}\ln(\delta)\right)^2}. \tag{3.15}$$

when we choose F = e and $\epsilon = 4\beta^2$, the Eq (3.15) becomes

$$\Re_8(t,x,y) = y_0 + \frac{\ln(\delta)^2\left(1 + \delta^{4(x\delta+y\mu+t\omega)}\ln(\delta)^4 + 2\delta^{2(x\delta+y\mu+t\omega)}\left(2\delta^2 - \ln(\delta)^2\right)\right)z_2}{\left(1 + \delta^{2(x\delta+y\mu+t\omega)}\ln(\delta)^2\right)^2}. \tag{3.16}$$

when we choose F = e and $\epsilon = -4\beta^2$, the Eq (3.15) becomes

$$\Re_9(t,x,y) = y_0 + \frac{\ln(\delta)^2\left(1+\delta^{4(x\delta+y\mu+t\omega)}\ln(\delta)^4 - 2\delta^{2(x\delta+y\mu+t\omega)}\left(2\delta^2 - \ln(\delta)^2\right)\right)z_2}{\left(-1+\delta^{2(x\delta+y\mu+t\omega)}\ln(\delta)^2\right)^2}. \tag{3.17}$$

Set 4.

$$y_1 = 0, z_1 = \delta, y_2 = -\frac{\epsilon\left(2\omega+\delta^2\mu\ln(\delta)^2\right)z_2}{\delta^2\mu}, F = \delta. \tag{3.18}$$

By putting set 3 in Eq (3.5), we obtain the exact solution as follows:

$$\Re_{10}(t,x,y) = y_0 + \frac{\left(-\frac{\delta^{-x\delta-y\mu-t\omega}\epsilon}{4\beta} + \beta\delta^{x\delta+y\mu+t\omega}\ln(\delta)^2\right)^2 z_2}{\left(\frac{\delta^{-x\delta-y\mu-t\omega}\epsilon}{4\beta\ln(\delta)} + \beta\delta^{x\delta+y\mu+t\omega}\ln(\delta)\right)^2} - \frac{\epsilon\left(2\omega+\delta^2\mu\ln(\delta)^2\right)z_2}{\delta^2\mu\left(\frac{\delta^{-x\delta-y\mu-t\omega}\epsilon}{4\beta\ln(\delta)} + \beta\delta^{x\delta+y\mu+t\omega}\ln(\delta)\right)^2}. \tag{3.19}$$

when we choose F = e and $\epsilon = 4\beta^2$, the Eq (3.19) becomes

$$\Re_{11}(t,x,y) = y_0 + \frac{\ln(\delta)^2\left(\delta^2\mu + \delta^{2+4x\delta+4y\mu+4t\omega}\mu\ln(\delta)^4 - 2\delta^{2(x\delta+y\mu+t\omega)}\left(4\omega+3\delta^2\mu\ln(\delta)^2\right)\right)z_2}{\mu\left(\delta+\delta^{1+2x\delta+2y\mu+2t\omega}\ln(\delta)^2\right)^2}. \tag{3.20}$$

when we choose F = e and $\epsilon = -4\beta^2$ the Eq (3.19) becomes

$$\Re_{12}(t,x,y) = y_0 + \frac{\ln(\delta)^2\left(\delta^2\mu + \delta^{2+4x\delta+4y\mu+4t\omega}\mu\ln(\delta)^4 + 2\delta^{2(x\delta+y\mu+t\omega)}\left(4\omega+3\delta^2\mu\ln(\delta)^2\right)\right)z_2}{\delta^2\mu\left(-1+\delta^{2(x\delta+y\mu+t\omega)}\ln(\delta)^2\right)^2}. \tag{3.21}$$

4. The modified sub-equation method

The basic steps of the modified sub-equation (MSE) method are as follows:
Step 01: The MSE method provides the solution of Eq (2.5) as follows:

$$\mathfrak{F}(\xi) = h_0 + \sum_{i=1}^{N} h_j M_j(\xi). \tag{4.1}$$

h_0, h_i (for i = 1, 2, . . . , N) are non-zero constants, with the condition $h_N \neq 0$, and the function $M(\xi)$ in Eq (4.1) satisfies the relation:

$$M'(\xi) = \sqrt{\sigma_2 M^4(\xi) + \sigma_1 M^2(\xi) + \sigma_0}. \tag{4.2}$$

Here, σ_0, σ_1, and $\sigma_2 \neq 0$ are real constants. The answer to Eq (4.2) is as follows:
Case 01: When $\sigma_0 = 0$, $\sigma_1 > 0$, and $\sigma_2 \neq 0$, then,

$$M^{01}(\xi) = \pm\sqrt{-\frac{\sigma_1}{\sigma_2}}\operatorname{sech}\left[\sqrt{\sigma_1}\xi + \rho\right]. \tag{4.3}$$

$$M^{02}(\xi) = \pm\sqrt{\frac{\sigma_1}{\sigma_2}}\operatorname{csch}\left[\sqrt{\sigma_1}\xi + \rho\right]. \tag{4.4}$$

Case 02: In case of constants B_1 and B_2, $\sigma_0 = 0$, $\sigma_1 > 0$, and $\sigma_2 = \pm 4A_1A_2$, then,

$$M^{03}(\xi) = \pm \frac{4\sqrt{\sigma_1}B_1}{\left(4B_1^2 - \sigma_2\right)\cosh\left(\sqrt{\sigma_1}(\xi+\rho)\right) + \left(4B_1^2 + \sigma_2\right)\sinh\left(\sqrt{\sigma_1}(\xi+\rho)\right)}. \tag{4.5}$$

Case 03: Consider $\sigma_0 = \frac{\sigma_1^2}{4\sigma_2}$, $\sigma_1 < 0$, and $\sigma_2 > 0$, then,

$$M^{04}(\xi) = \pm\sqrt{-\frac{\sigma_1}{2\sigma_2}}\tanh\left[\sqrt{\frac{-\sigma_1}{2}}\xi + \rho\right]. \tag{4.6}$$

$$M^{05}(\xi) = \pm\sqrt{-\frac{\sigma_1}{2\sigma_2}}\coth\left[\sqrt{\frac{-\sigma_1}{2}}\xi + \rho\right]. \tag{4.7}$$

$$M^{06}(\xi) = \pm\sqrt{-\frac{\sigma_1}{2\sigma_2}}\left[\tanh\left(\sqrt{-2\sigma_1}\xi + \rho\right) + \iota\,\mathrm{sech}\left(\sqrt{-2\sigma_1}\xi + \rho\right)\right]. \tag{4.8}$$

$$M^{07}(\xi) = \pm\sqrt{-\frac{\sigma_1}{2\sigma_2}}\left[\tanh\left(\sqrt{-2\sigma_1}\xi + \rho\right) + \iota\,\mathrm{sech}\left(\sqrt{-2\sigma_1}\xi + \rho\right)\right]^{-1}. \tag{4.9}$$

Case 04: When $\sigma_0 = 0$, $\sigma_1 < 0$, and $\sigma_2 \neq 0$, then,

$$M^{08}(\xi) = \pm\sqrt{-\frac{\sigma_1}{2\sigma_2}}\sec\left[\sqrt{-\sigma_1}\xi + \rho\right]. \tag{4.10}$$

$$M^{09}(\xi) = \pm\sqrt{-\frac{\sigma_1}{2\sigma_2}}\csc\left[\sqrt{-\sigma_1}\xi + \rho\right]. \tag{4.11}$$

Case 05: Consider $\sigma_0 = \frac{\sigma_1^2}{4\sigma_2}$, $\sigma_1 > 0$, and $\sigma_2 > 0$, then,

$$M^{10}(\xi) = \pm\sqrt{\frac{\sigma_1}{2\sigma_2}}\tan\left[\sqrt{\frac{\sigma_1}{2}}\xi + \rho\right]. \tag{4.12}$$

$$M^{11}(\xi) = \pm\sqrt{\frac{\sigma_1}{2\sigma_2}}\cot\left[\sqrt{\frac{\sigma_1}{2}}\xi + \rho\right]. \tag{4.13}$$

$$M^{12}(\xi) = \pm\sqrt{\frac{\sigma_1}{2\sigma_2}}\left[\tan\left(\sqrt{2\sigma_1}\xi + \rho\right) + \sec\left(\sqrt{2\sigma_1}\xi + \rho\right)\right]. \tag{4.14}$$

$$M^{13}(\xi) = \pm\sqrt{\frac{\sigma_1}{2\sigma_2}}\left[\tan\left(\sqrt{2\sigma_1}\xi + \rho\right) + \sec\left(\sqrt{2\sigma_1}\xi + \rho\right)\right]^{-1}. \tag{4.15}$$

Case 06: If $\sigma_0 = 0$, $\sigma_1 > 0$, then,

$$M^{14}(\xi) = \pm\frac{4\sigma_1 \mathrm{e}^{\sqrt{\sigma_1}\xi+\rho}}{\mathrm{e}^{2\sqrt{\sigma_1}\xi+\rho} - 4\sigma_1\sigma_2}. \tag{4.16}$$

$$M^{15}(\xi) = \pm\frac{4\sigma_1 \mathrm{e}^{\sqrt{\sigma_1}\xi+\rho}}{1 - 4\sigma_1\sigma_2\mathrm{e}^{2\sqrt{\sigma_1}\xi+\rho}}. \tag{4.17}$$

Case 07: When $\sigma_0 = \sigma_1 = 0$, $\sigma_2 > 0$, then,

$$M^{16}(\xi) = \pm\frac{1}{\sqrt{\sigma_2}\xi + \rho}. \tag{4.18}$$

Case 08: If $\sigma_0 = \sigma_1 = 0$, $\sigma_2 > 0$, then,

$$M^{17}(\xi) = \pm\frac{\iota}{\sqrt{-\sigma_2}\xi + \rho}. \tag{4.19}$$

Step 02: By balancing the non-linear term and the term with the highest order derivative in Eq (2.5), the positive integer N is determined for Eq (4.1).
Step 03: After inserting Eqs (4.1) and (4.2) in Eq (2.5), and since $M^i(\xi) \neq 0$, for (i = 1,2,3,..., N) as a result of this substitution, we get a polynomial of $M^i(\xi)$. Equivalently, we set all terms with the same power equal to zero. Then, by solving this set of nonlinear algebraic systems and with the help of Eqs (4.2) and (2.2), the solutions of Eq (1.7) may be determined.

4.1. Solution by the modified sub-equation method

To find the exact solution of Eq (2.5), first we find the value of the positive integer N=2 and add the value of N to Eq (4.1). Then, Eq (4.1) will become as follows:

$$\Re(\xi) = h_0 + h_1 M(\xi) + h_2 M(\xi)^2. \tag{4.20}$$

By inserting Eq (4.20) into Eq (1.7), together with Eqs (2.2) and (4.2), we have a polynomial in terms of $M^j(\xi)$. This creates a system of algebraic equations when we aggregate all terms of the same power and equal them to zero. The values of unknown constants are obtained.

Set 01:

$$\mu = \frac{\sqrt{-\frac{1}{3\sigma_0\sigma_2 - \sigma_1^2}}\ \omega}{\delta^2},\quad h_0 = \frac{\left(\sqrt{-\frac{1}{3\sigma_0\sigma_2 - \sigma_1^2}}\ \sigma_1 + 1\right)\delta}{3\sqrt{-\frac{1}{3\sigma_0\sigma_2 - \sigma_1^2}}},\quad h_1 = 0,\quad h_2 = \delta\sigma_2. \tag{4.21}$$

By putting Set 1 in Eq (4.20), we get the exact solutions as follows:
Case 01: When $\sigma_0 = 0\sigma_1 > 0$, and $\sigma_2 \neq 0$, then,

$$\Re_{01}(t, y, x) = \frac{\left(\sqrt{-\frac{1}{3\sigma_0\sigma_2 - \sigma_1^2}}\,\sigma_1 + 1\right)\delta}{3\sqrt{-\frac{1}{3\sigma_0\sigma_2 - \sigma_1^2}}} - \delta\sigma_1 \mathrm{sech}\left(\sqrt{\sigma_1}\,\xi + \rho\right)^2. \tag{4.22}$$

$$\Re_{02}(t, y, x) = \frac{\left(\sqrt{-\frac{1}{3\sigma_0\sigma_2 - \sigma_1^2}}\,\sigma_1 + 1\right)\delta}{3\sqrt{-\frac{1}{3\sigma_0\sigma_2 - \sigma_1^2}}} + \delta\sigma_1 \mathrm{csch}\left(\sqrt{\sigma_1}\,\xi + \rho\right)^2. \tag{4.23}$$

Case 02: In case of constants $B_1$and B_2, $\sigma_0 = 0$, $\sigma_1 > 0$, and $\sigma_2 = \pm 4A_1A_2$, then,

$$\Re_{03}(t,y,x)=\frac{16\delta\sigma_2\sigma_1A_1^2}{\left(\left(4A_1^2-\sigma_2\right)\cosh\left(\sqrt{\sigma_1}\ (\xi+\rho)\right)+\left(4A_1^2+\sigma_2\right)\sinh\left(\sqrt{\sigma_1}\ (\xi+\rho)\right)\right)^2}+\frac{\left(\sqrt{-\frac{1}{3\sigma_0\sigma_2-\sigma_1^2}}\,\sigma_1+1\right)\delta}{3\sqrt{-\frac{1}{3\sigma_0\sigma_2-\sigma_1^2}}}. \tag{4.24}$$

Case 03: Consider $\sigma_0=\frac{\sigma_1^2}{4\sigma_2}$, $\sigma_1<0$, and $\sigma_2>0$, then,

$$\Re_{04}(t,y,x)=\frac{\left(\sqrt{-\frac{1}{3\sigma_0\sigma_2-\sigma_1^2}}\,\sigma_1+1\right)\delta}{3\sqrt{-\frac{1}{3\sigma_0\sigma_2-\sigma_1^2}}}-\frac{\delta\sigma_1\tanh\left(\frac{\sqrt{-2\sigma_1}\,\xi}{2}+\rho\right)^2}{2}. \tag{4.25}$$

$$\Re_{05}(t,y,x)=\frac{\left(\sqrt{-\frac{1}{3\sigma_0\sigma_2-\sigma_1^2}}\,\sigma_1+1\right)\delta}{3\sqrt{-\frac{1}{3\sigma_0\sigma_2-\sigma_1^2}}}-\frac{\delta\sigma_1\coth\left(\frac{\sqrt{-2\sigma_1}\,\xi}{2}+\rho\right)^2}{2}. \tag{4.26}$$

$$\Re_{06}(t,y,x)=\frac{\left(\sqrt{-\frac{1}{3\sigma_0\sigma_2-\sigma_1^2}}\,\sigma_1+1\right)\delta}{3\sqrt{-\frac{1}{3\sigma_0\sigma_2-\sigma_1^2}}}-\frac{\delta\sigma_1\left(\tanh\left(\sqrt{-2\sigma_1}\,\xi+\rho\right)+\mathrm{I}\,\mathrm{sech}\left(\sqrt{-2\sigma_1}\,\xi+\rho\right)\right)^2}{2}. \tag{4.27}$$

$$\Re_{07}(t,y,x)=\frac{\left(\sqrt{-\frac{1}{3\sigma_0\sigma_2-\sigma_1^2}}\,\sigma_1+1\right)\delta}{3\sqrt{-\frac{1}{3\sigma_0\sigma_2-\sigma_1^2}}}-\frac{\delta\sigma_1}{2\left(\tanh\left(\sqrt{-2\sigma_1}\,\xi+\rho\right)+\mathrm{I}\,\mathrm{sech}\left(\sqrt{-2\sigma_1}\,\xi+\rho\right)\right)^2}. \tag{4.28}$$

Case 04: When $\sigma_0=0$, $\sigma_1<0$, and $\sigma_2\neq0$, then,

$$\Re_{08}(t,y,x)=\frac{\left(\sqrt{-\frac{1}{3\sigma_0\sigma_2-\sigma_1^2}}\,\sigma_1+1\right)\delta}{3\sqrt{-\frac{1}{3\sigma_0\sigma_2-\sigma_1^2}}}-\frac{\delta\sigma_1\sec\left(\sqrt{-\sigma_1}\,\xi+\rho\right)^2}{2}. \tag{4.29}$$

$$\Re_{09}(t,y,x)=\frac{\left(\sqrt{-\frac{1}{3\sigma_0\sigma_2-\sigma_1^2}}\,\sigma_1+1\right)\delta}{3\sqrt{-\frac{1}{3\sigma_0\sigma_2-\sigma_1^2}}}-\frac{\delta\sigma_1\csc\left(\sqrt{-\sigma_1}\,\xi+\rho\right)^2}{2}. \tag{4.30}$$

Case 05: Consider $\sigma_0=\frac{\sigma_1^2}{4\sigma_2}$, $\sigma_1>0$, and $\sigma_2>0$, then,

$$\Re_{10}(t,y,x)=\frac{\left(\sqrt{-\frac{1}{3\sigma_0\sigma_2-\sigma_1^2}}\,\sigma_1+1\right)\delta}{3\sqrt{-\frac{1}{3\sigma_0\sigma_2-\sigma_1^2}}}+\frac{\delta\sigma_1\tan\left(\frac{\sqrt{2}\,\sqrt{\sigma_1}\,\xi}{2}+\rho\right)^2}{2}. \tag{4.31}$$

$$\Re_{11}(t,y,x)=\frac{\left(\sqrt{-\frac{1}{3\sigma_0\sigma_2-\sigma_1^2}}\,\sigma_1+1\right)\delta}{3\sqrt{-\frac{1}{3\sigma_0\sigma_2-\sigma_1^2}}}+\frac{\delta\sigma_1\cot\left(\frac{\sqrt{2}\,\sqrt{\sigma_1}\,\xi}{2}+\rho\right)^2}{2}. \tag{4.32}$$

$$\Re_{12}(t,y,x)=\frac{\left(\sqrt{-\frac{1}{3\sigma_0\sigma_2-\sigma_1^2}}\,\sigma_1+1\right)\delta}{3\sqrt{-\frac{1}{3\sigma_0\sigma_2-\sigma_1^2}}}+\frac{\delta\sigma_1\left(\tan\left(\sqrt{2}\,\sqrt{\sigma_1}\,\xi+\rho\right)+\sec\left(\sqrt{2}\,\sqrt{\sigma_1}\,\xi+\rho\right)\right)^2}{2}. \tag{4.33}$$

$$\Re_{13}(t,y,x)=\frac{\left(\sqrt{-\frac{1}{3\sigma_0\sigma_2-\sigma_1^2}}\,\sigma_1+1\right)\delta}{3\sqrt{-\frac{1}{3\sigma_0\sigma_2-\sigma_1^2}}}+\frac{\delta\sigma_1}{2\left(\tan\left(\sqrt{2}\,\sqrt{\sigma_1}\,\xi+\rho\right)+\sec\left(\sqrt{2}\,\sqrt{\sigma_1}\,\xi+\rho\right)\right)^2}. \tag{4.34}$$

Case 06: If $\sigma_0=0$, $\sigma_1>0$, then,

$$\Re_{14}(t,y,x)=\frac{\left(\sqrt{-\frac{1}{3\sigma_0\sigma_2-\sigma_1^2}}\,\sigma_1+1\right)\delta}{3\sqrt{-\frac{1}{3\sigma_0\sigma_2-\sigma_1^2}}}+\frac{16\delta\sigma_2\sigma_1^2\left(\mathrm{e}^{\sqrt{\sigma_1}\,\xi+\rho}\right)^2}{\left(\mathrm{e}^{2\sqrt{\sigma_1}\,\xi+\rho}-4\sigma_1\sigma_2\right)^2}. \tag{4.35}$$

$$\Re_{15}(t,y,x)=\frac{\left(\sqrt{-\frac{1}{3\sigma_0\sigma_2-\sigma_1^2}}\,\sigma_1+1\right)\delta}{3\sqrt{-\frac{1}{3\sigma_0\sigma_2-\sigma_1^2}}}+\frac{16\delta\sigma_2\sigma_1^2\left(\mathrm{e}^{\sqrt{\sigma_1}\,\xi+\rho}\right)^2}{\left(1-4\sigma_1\sigma_2\mathrm{e}^{2\sqrt{\sigma_1}\,\xi+\rho}\right)^2}. \tag{4.36}$$

Case 07: When $\sigma_0=\sigma_1=0$, $\sigma_2>0$, then,

$$\Re_{16}(t,y,x)=\frac{\left(\sqrt{-\frac{1}{3\sigma_0\sigma_2-\sigma_1^2}}\,\sigma_1+1\right)\delta}{3\sqrt{-\frac{1}{3\sigma_0\sigma_2-\sigma_1^2}}}+\frac{\delta\sigma_2}{\left(\sqrt{\sigma_2}\,\xi+\rho\right)^2}. \tag{4.37}$$

Case 08: If $\sigma_0=\sigma_1=0$, $\sigma_2>0$, then,

$$\Re_{17}(t,y,x)=\frac{\left(\sqrt{-\frac{1}{3\sigma_0\sigma_2-\sigma_1^2}}\,\sigma_1+1\right)\delta}{3\sqrt{-\frac{1}{3\sigma_0\sigma_2-\sigma_1^2}}}-\frac{\delta\sigma_2}{\left(\sqrt{-\sigma_2}\,\xi+\rho\right)^2}. \tag{4.38}$$

5. Results and discussion

In this section, we have selected specific values for the physical parameters to illustrate the significance of the new optical solutions for the current governing equation. The effect of both parameters x and t on the existing soliton solutions is portrayed through two-dimensional (2D) and three-dimensional (3D) graphs, streamline plots, and polar plots. Figures 1–8 present 3D, 2D, streamline plots, and polar plots, illustrating the behavior of the current solutions.

Figure 1 illustrates the spatiotemporal dynamics of the bright soliton solution $Q_{01}(t,y,x)$, providing a graphical visualization of the derived solution of Eq (3.7), The figure includes (a) a 3D surface plot, (b) 2D surface plot, (c) streamline plot, and (d) polar plot , illustrating solution's evolution with varying

values of the temporal parameters, namely $\rho = 1, \mu = 1, \omega = 1, \beta_2 = 1, \delta = 2.1, \eta = 0.1, B = 1, y = -1, \alpha_0 = -1$, and $A = 2$. Bright solitons are characterized by localized peaks in intensity, emerging from a zero or near-zero background due to the interplay between dispersion and nonlinearity.

Figure 2 represents the dark soliton solution $Q_{04}(t, y, x)$, providing a graphical visualization of the derived solution of Eq (3.11) by illustrating its evolution through (a) a 3D surface plot, (b) 2D surface plot, (c) streamline plot, and (d) polar plot, for varying values of the temporal parameters, namely $\rho = 1, \mu = 1, \omega = 0.6, \beta_2 = 1, \delta = 2.5, \eta = 0.1, B = 1, y = -1.5, \alpha_0 = -1$, and $A = 3$. of the solution. A dark soliton is a type of localized wave solution that appears as a dip or notch in the amplitude of a continuous wave background. It is a stable, self-reinforcing structure that occurs in nonlinear dispersive media.

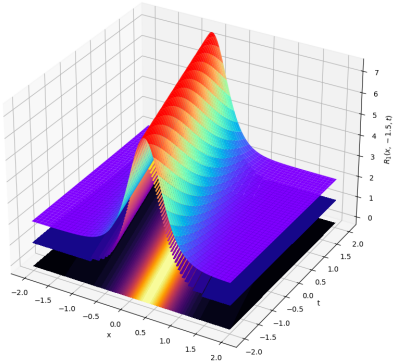

(a) 3D surface

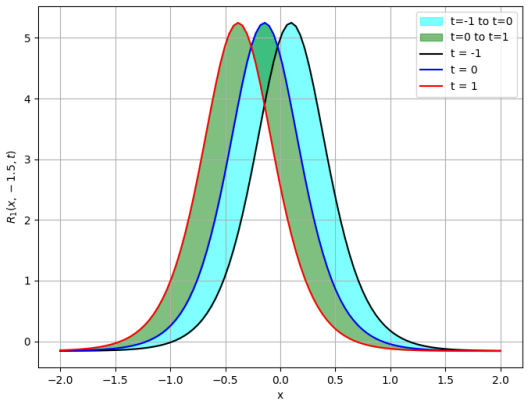

(b) 2D surface

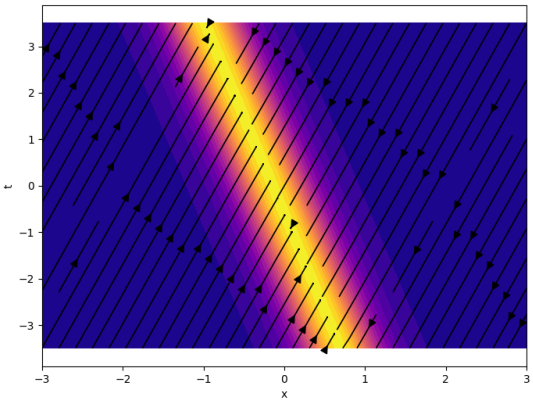

(c) Streamline plot

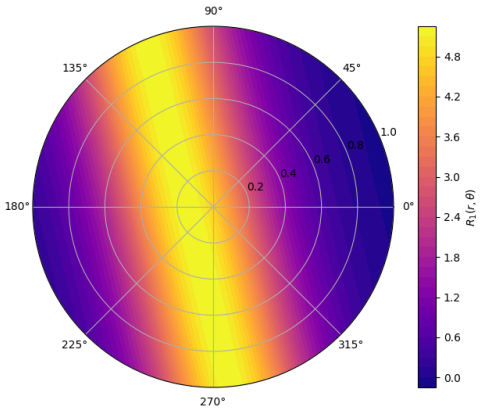

(d) Polar plot

Figure 1. Graphical visualization of the derived solution of Eq (3.7) as a (a) 3D surface plot, (b) 2D surface plot, (c) streamline plot, and (d) polar plot of $Q_{01}(t, y, x)$ with parameters $\rho = 1, \mu = 1, \omega = 1, \beta_2 = 1, \delta = 2.1, \eta = 0.1, B = 1, y = -1, \alpha_0 = -1$, and $A = 2$.

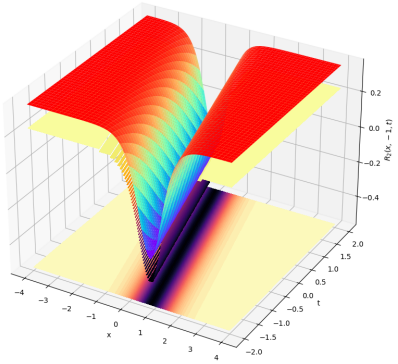

(a) 3D surface

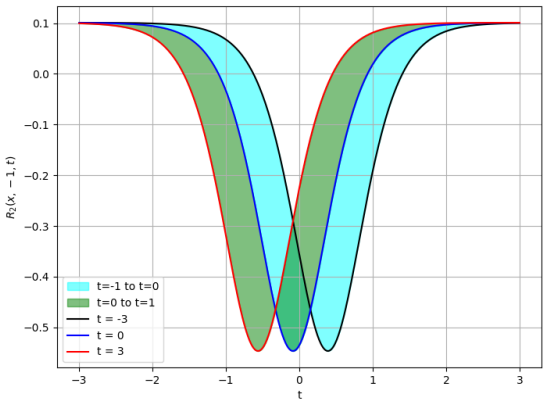

(b) 2D surface

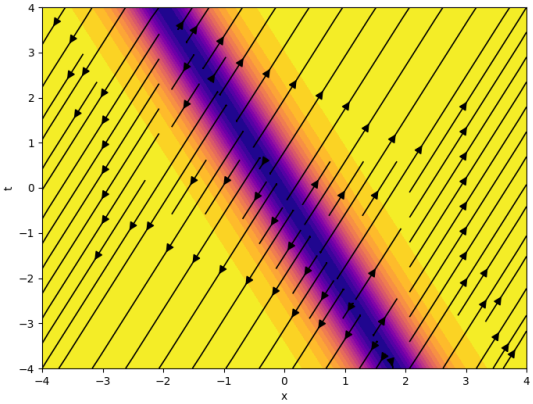

(c) Streamline plot

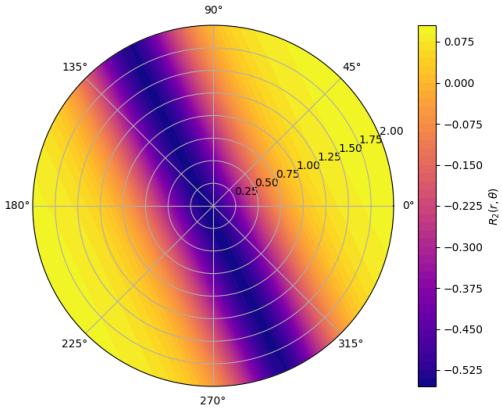

(d) Polar plot

Figure 2. Graphical visualization of the derived solution of Eq (3.11) as a (a) 3D surface plot, (b) 2D surface plot, (c) streamline plot, and (d) polar plot of $Q_{04}(t, y, x)$ with parameters $\rho = 1,\ \mu = 1,\ \omega = 0.6,\ \beta_2 = 1,\ \delta = 2.5,\ \eta = 0.1,\ B = 1,\ y = -1.5,\ \alpha_0 = -1$, and $A = 3$.

Figure 3 provides a detailed visualization of the kink-type soliton solution $Q_{07}(t, y, x)$ for varying values of the temporal parameter t and $\rho = 1, \mu = 1, \omega = 0.6, \beta_2 = 1, \delta = 2.1, \eta = 0.1, B = 1, y = 1, \alpha_0 = 1$, and $A = 1.1$. A kink soliton is a topological soliton that represents a smooth but localized change from one asymptotic state to another, typically moving through space with constant shape and speed. It connects two different constant values of a field at spatial infinity and is non-periodic and stable. The soliton profile exhibits a smooth, monotonic rise, demonstrating its stability and persistent structure over time. The resulting profile becomes noticeably sharper and more abrupt, with enhanced gradient steepness and increased localization. This reflects the influence of fractional-order dynamics in intensifying nonlinear effects and compressing the soliton structure.

Similarly, Figure 4 illustrates the spatiotemporal dynamics of the bright soliton solution $\Re_{01}(t, y, x)$, providing a graphical visualization of the derived solution of Eq (4.22) through (a) a 3D surface plot,

(b) a 2D surface plot, (c) a streamline plot, and (d) a polar plot, illustrating its evolution with varying values of the temporal parameters $\sigma_0 = 0, \sigma_1 = 0.4, \sigma_2 = 1, \delta = -0.9, \omega = 0.5, y = 0.3, \rho = 0.8$, and $\mu = 1.54$.

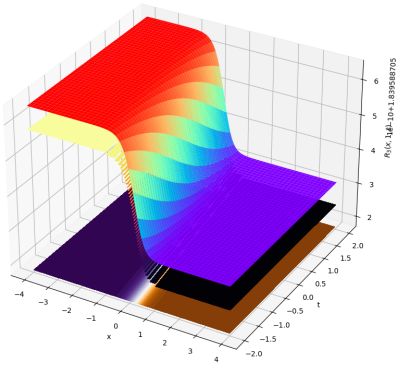

(a) 3D surface

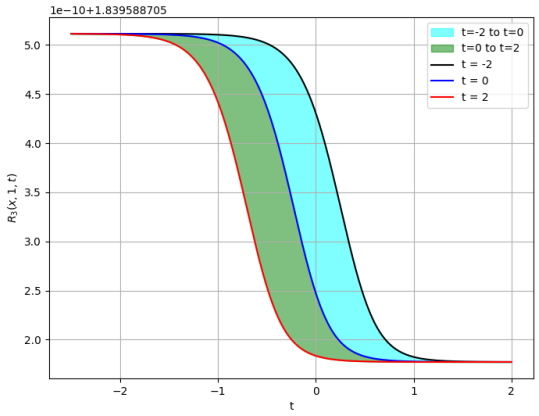

(b) 2D surface

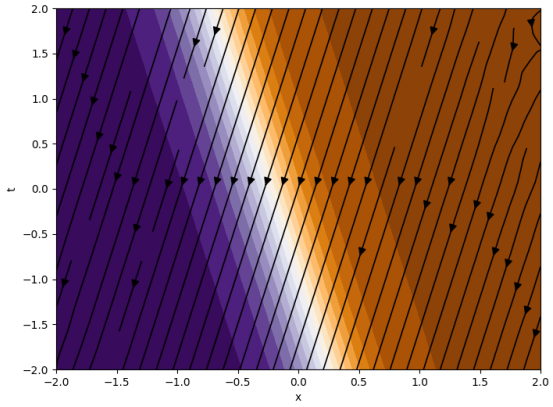

(c) Streamline plot

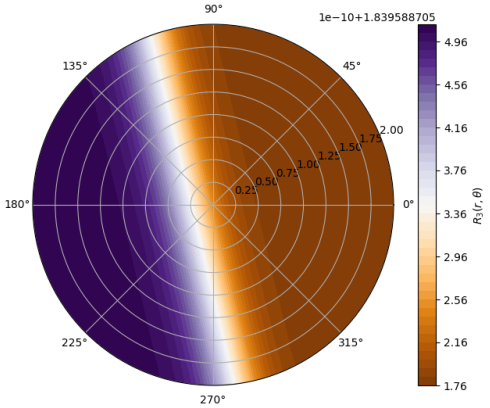

(d) Polar plot

Figure 3. Graphical visualization of the derived solution of Eq (3.15) as a (a) 3D surface plot, (b) 2D surface plot, (c) streamline plot, and (d) polar plot of $Q_{07}(t, y, x)$ with parameters $\rho = 1,\ \mu = 1,\ \omega = 0.6,\ \beta_2 = 1,\ \delta = 2.1,\ \eta = 0.1,\ B = 1,\ y = 1,\ \alpha_0 = 1$, and $A = 1.1$.

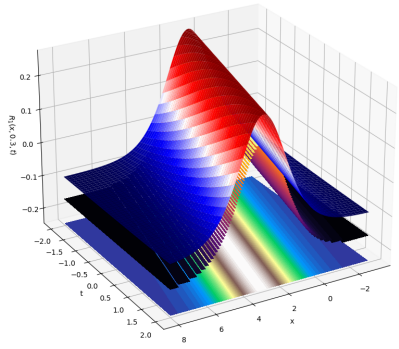

(a) 3D surface

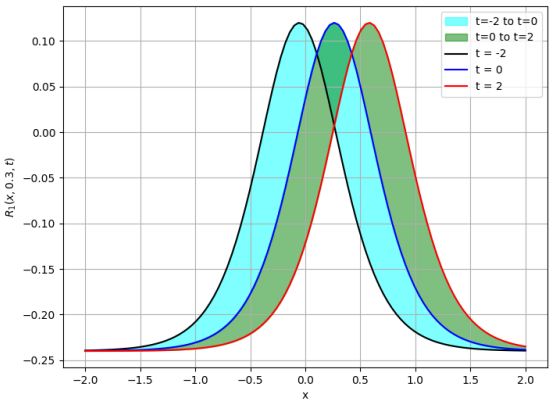

(b) 2D surface

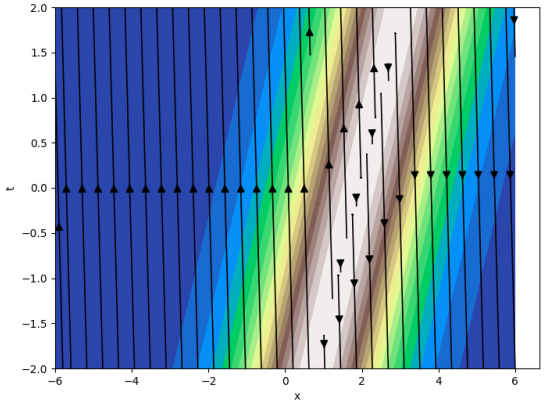

(c) Streamline plot

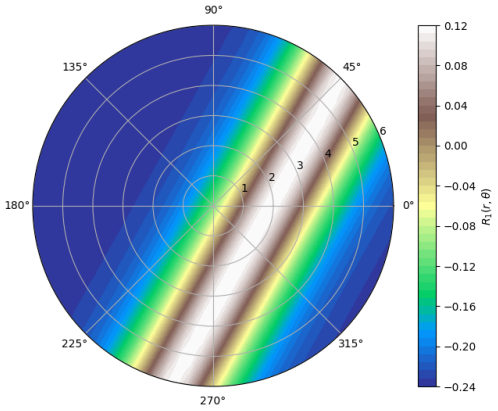

(d) Polar plot

Figure 4. Graphical visualization of the derived solution of Eq (4.22) as a bright soliton, including (a) a 3D surface plot, (b) a 2D surface plot, (c) a streamline plot, and (d) a polar plot of $\Re_{01}(t, y, x)$ with parameters $\sigma_0 = 0$, $\sigma_1 = 0.4$, $\sigma_2 = 1$, $\delta = -0.9$, $\omega = 0.5$, $y = 0.3$, $\rho = 0.8$, and $\mu = 1.54$.

Figure 5 illustrates the spatiotemporal dynamics of the multiple dark-bright soliton solution of $|\Re_{04}(t, y, x)|$, illustrating its evolution for varying values of the temporal parameter t and $\sigma_0 = 0.009, \sigma_1 = -0.15, \sigma_2 = 0.6, \delta = 0.8, \omega = 0.8, y = 0.2, \rho = 0.6$, and $\mu = 2.94I$. A dark-bright soliton is a combination of a dark soliton and a bright soliton. It has the characteristics of both solutions. The soliton maintains a well-defined structure as it propagates, combining localized dips and peaks, a signature of the mixed dark-bright soliton class.

Similarly, Figure 6 illustrates the spatiotemporal dynamics of the bright soliton solution of $|\Re_{06}(t, y, x)|$, illustrating its evolution with varying values of the temporal parameter t and $\sigma_0 = -0.1, \sigma_1 = 1, \sigma_2 = 0.1, \delta = 0.8, \omega = 0.3, y = 1, \rho = 0.8$, and $\mu = 6.62I$.

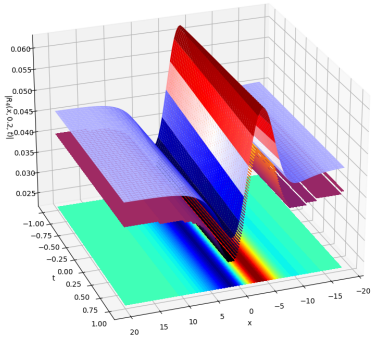

(a) 3D surface

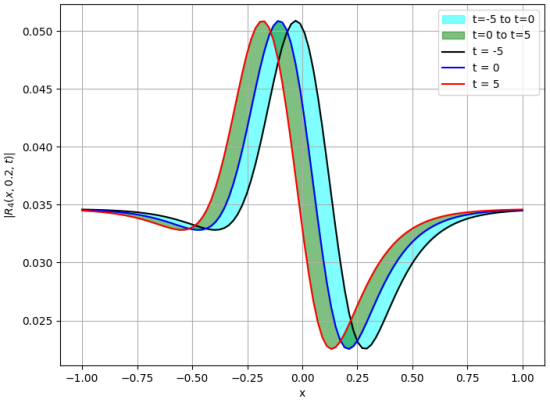

(b) 2D surface

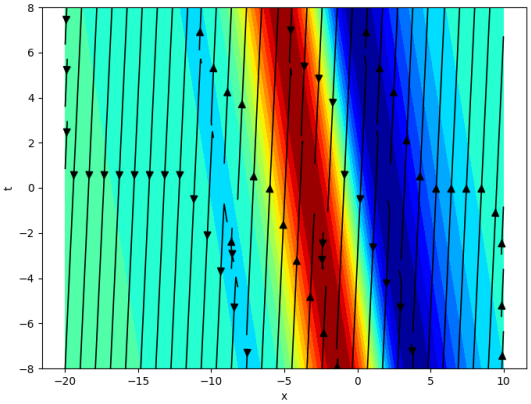

(c) Streamline plot

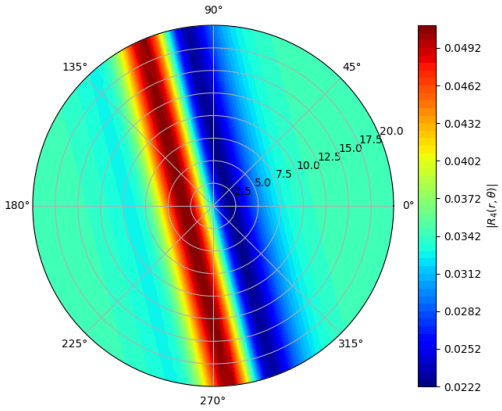

(d) Polar plot

Figure 5. Graphical visualization of the derived solution of Eq (4.25) yielding a dark-bright soliton, including (a) 3D surface plot, (b) 2D surface plot, (c) streamline plot, and (d) polar plot of $|\Re_{04}(t, y, x)|$ with parameters $\sigma_0 = 0.009$, $\sigma_1 = -0.15$, $\sigma_2 = 0.6$, $\delta = 0.8$, $\omega = 0.8$, $y = 0.2$, $\rho = 0.6$, and $\mu = 2.94I$.

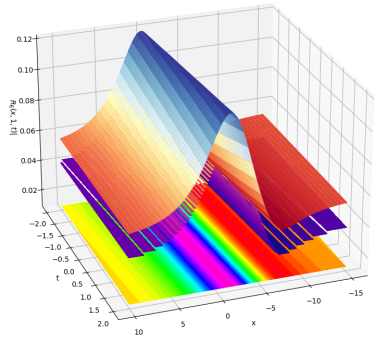

(a) 3D surface

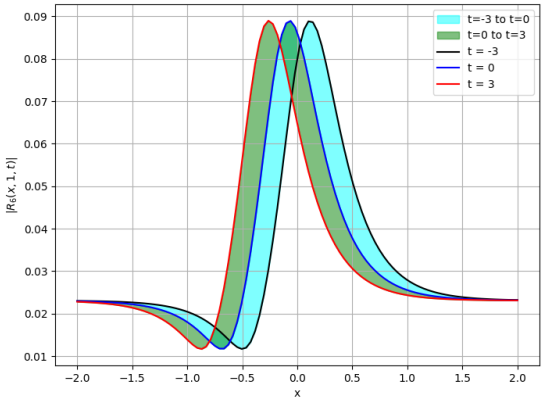

(b) 2D surface

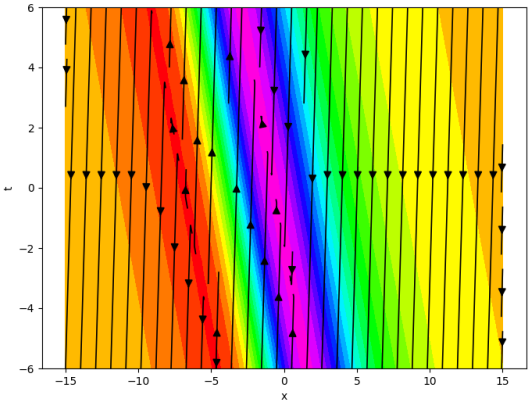

(c) Streamline plot

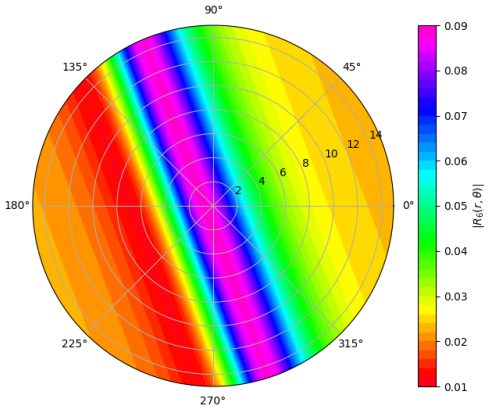

(d) Polar plot

Figure 6. Graphical visualization of the derived solution of Eq (4.27) yielding a bright-dark soliton, including (a) 3D surface plot, (b) 2D surface plot, (c) streamline plot, and (d) polar plot of $|\Re_{06}(t, y, x)|$ with parameters $\sigma_0 = -0.1$, $\sigma_1 = 1$, $\sigma_2 = 0.1$, $\delta = 0.8$, $\omega = 0.3$, $y = 1$, $\rho = 0.8$, and $\mu = 6.62I$.

Figure 7 represents the periodic wave solution $\Re_{07}(t, y, x)|$ by using suitable parametric values: $\sigma_0 = 0.05, \sigma_1 = 1, \sigma_2 = 0.1, \delta = 1.2, \omega = 1.5, y = 1, \rho = 0.6$, and $\mu = 29.62I$. Periodic waves are defined as a standard soliton, which is a single, localized pulse that maintains its shape during propagation. A periodic soliton repeats itself in space or time and typically arises in nonlinear dispersive systems.

Figure 8 represents the dark soliton solution $\Re_{15}(t, y, x)$ using suitable parametric values: $\sigma_0 = 0, \sigma_1 = 0.9, \sigma_2 = -0.1, \delta = 0.6, \omega = 0.2, y = 0.5, \rho = 0.4$, and $\mu = 0.61$. A dark soliton is a type of localized wave solution that appears as a dip or notch in the amplitude of a continuous wave background. It is a stable, self-reinforcing structure that occurs in nonlinear dispersive media.

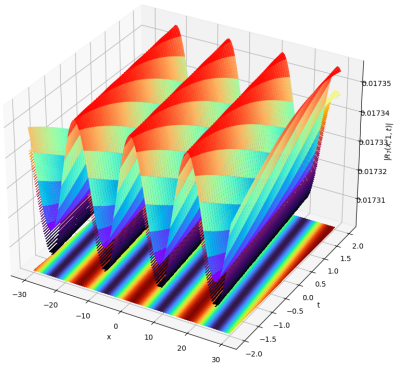

(a) 3D surface

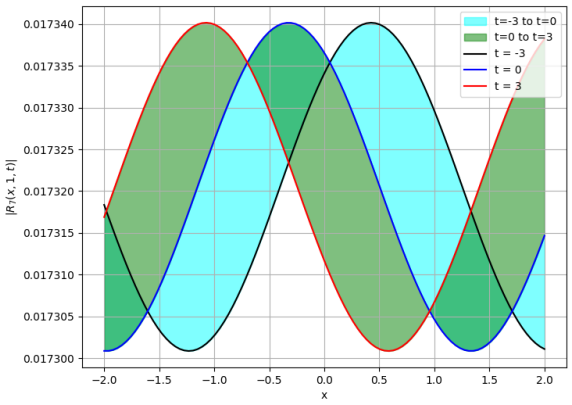

(b) 2D surface

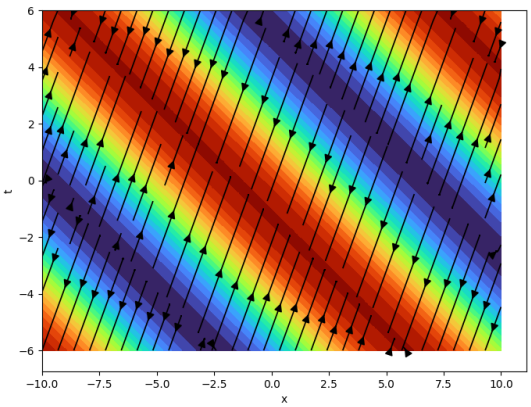

(c) Streamline plot

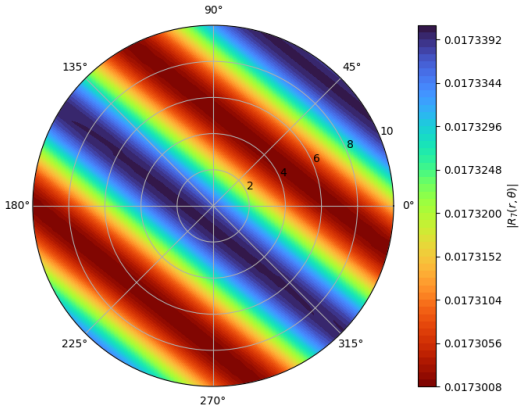

(d) Polar plot

Figure 7. Graphical visualization of the derived solution of Eq (4.28) showing a periodic soliton structure, including (a) 3D surface plot, (b) 2D surface plot, (c) streamline plot, and (d) polar plot of $|\Re_{07}(t, y, x)|$ with parameters $\sigma_0 = 0.05$, $\sigma_1 = 1$, $\sigma_2 = 0.1$, $\delta = 1.2$, $\omega = 1.5$, $y = 1$, $\rho = 0.6$, and $\mu = 29.62I$.

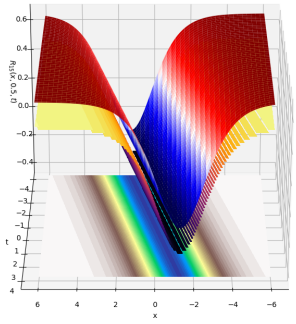

(a) 3D surface

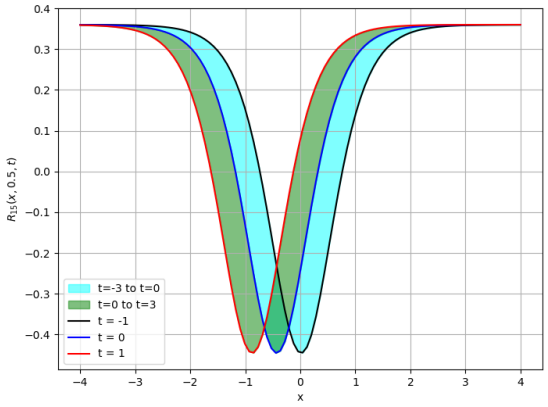

(b) 2D surface

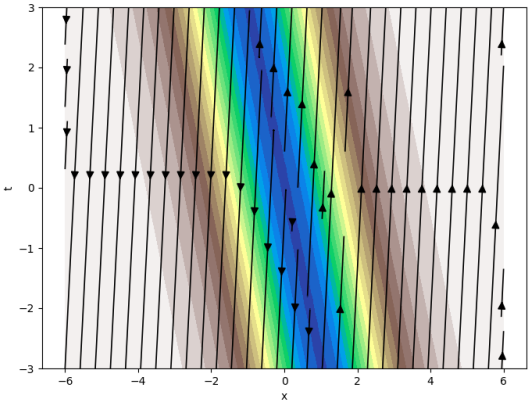

(c) Streamline plot

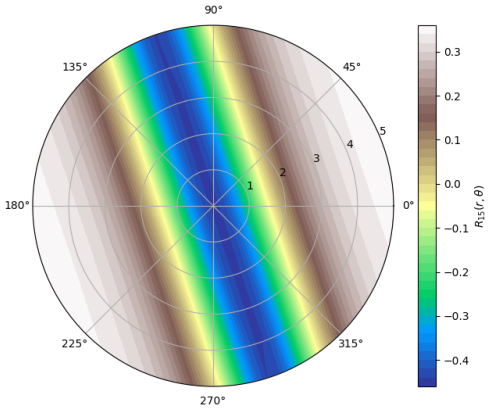

(d) Polar plot

Figure 8. Graphical visualization of the derived solution of Eq (4.38) showing a dark soliton structure, including (a) 3D surface plot, (b) 2D surface plot, (c) streamline plot, and (d) polar plot of $\Re_{15}(t, y, x)$ with parameters $\sigma_0 = 0$, $\sigma_1 = 0.9$, $\sigma_2 = -0.1$, $\delta = 0.6$, $\omega = 0.2$, $y = 0.5$, $\rho = 0.4$, and $\mu = 0.61$.

6. Conclusions

In conclusion, we introduced two new methods to find exact solutions for NLPDEs, specifically focusing on the (2+1)-dimensional integrable Schwarz–Korteweg–de Vries equation. The NLPDE was converted into a PDE through traveling wave transformation, after which the generalized Arnous and the modified sub-equation methods were applied to the proposed Eq (1.7). The solutions demonstrate the applicability of our model. These methodologies resulted in a wide range of dark, bright, kink, dark-bright, and bright-dark solitary waves. These results were graphically represented through 3D surface (including density and contour plots), 2D surface plots, streamline plots, and polar plots. Our proposed method presents a systematic and efficient technique to solve NLPDEs, especially by showing

its application in the Schwarz–Korteweg–de Vries equation. We tested the methods using Maple and Python, which confirmed the precision and usefulness in nonlinear differential equations. In the future, we can apply these methods to different NLPDEs to verify their applicability and precision in various mathematical fields. Moreover, our key focus is to develop numeric models to achieve high precision in the real-time modeling of real systems. Evaluating these methods against a wide range of benchmark problems and contrasting their performance with other methods can help us in assessing their stability and sensitivity. Moreover, the scope of this study by can be widened including lump interactions, researching multi-soliton situations, and analyzing the dynamics of breather-type rogue waves. Such additions might improve the practical application and relevance of this research.

Author contributions

Khizar Farooq: Formal analysis, Methodology, Writing–review and editing; Ejaz Hussain: Software, Methodology, Writing–review and editing; Hamza Ali Abujabal: Investigation, Supervision, Writing–review and editing; Fehaid Salem Alshammari: Validation, Funding, Project administration, Writing–review and editing.

Use of Generative-AI tools declaration

The authors declare they have not used Artificial Intelligence (AI) tools in the creation of this article.

Funding

This work was supported and funded by the Deanship of Scientific Research at Imam Mohammad Ibn Saud Islamic University (IMSIU) (grant number IMSIU-DDRSP2503).

Conflict of interest

The authors declare no conflicts of interest to report regarding the present study.

Data Availability

The data that support the findings of this study are available from the corresponding author upon reasonable request.

References

1. S. M. Rayhanul Islam, K. Khan, M. A. Akbar, Optical soliton solutions, bifurcation, and stability analysis of the Chen–Lee–Liu model, *Results Phys.*, **51** (2023), 106620. https://doi.org/10.1016/j.rinp.2023.106620
2. E. Hussain, Y. Arafat, S. Malik, F. S. Alshammari, The (2+1)-dimensional chiral nonlinear Schrödinger equation: extraction of soliton solutions and sensitivity analysis, *Axioms*, **14** (2025), 422. https://doi.org/10.3390/axioms14060422

3. J. T. Stuart, On the non-linear mechanics of hydrodynamic stability, *J. Fluid Mech.*, **4** (1958), 1–21. https://doi.org/10.1017/S0022112058000276

4. K. Farooq, E. Hussain, U. Younas, H. Mukalazi, T. M. Khalaf, A. Mutlib, et al., Exploring the wave's structures to the nonlinear coupled system arising in surface geometry, *Sci. Rep.*, **15** (2025), 11624. https://doi.org/10.1038/s41598-024-84657-w

5. W. F. Ames, *Nonlinear partial differential equations in engineering*, Academic Press, 1965.

6. M. A. Mustafa, M. A. S. Murad, Soliton solutions to the time-fractional Kudryashov equation: applications of the new direct mapping method, *Mod. Phys. Lett. B*, **39** (2025), 2550147. https://doi.org/10.1142/S0217984925501477

7. E. Hussain, A. H. Tedjani, K. Farooq, Beenish, Modeling and exploration of localized wave phenomena in optical fibers using the generalized Kundu–Eckhaus equation for femtosecond pulse transmission, *Axioms*, **14** (2025), 513. https://doi.org/10.3390/axioms14070513

8. W. B. Rabie, H. M. Ahmed, M. Mirzazadeh, A. Akbulut, M. S. Hashemi, Investigation of solitons and conservation laws in an inhomogeneous optical fiber through a generalized derivative nonlinear Schrödinger equation with quintic nonlinearity, *Opt. Quant. Electron.*, **55** (2023), 825. https://doi.org/10.1007/s11082-023-05070-7

9. K. Farooq, A. H. Tedjani, Z. Li, E. Hussain, Soliton dynamics of the nonlinear Kodama equation with M-truncated derivative via two innovative schemes: the generalized Arnous method and the Kudryashov method, *Fractal Fract.*, **9** (2025), 436. https://doi.org/10.3390/fractalfract9070436

10. M. A. Akbar, F. A. Abdullah, M. T. Islam, M. A. Al Sharif, M. S. Osman, New solutions of the soliton type of shallow water waves and superconductivity models, *Results Phys.*, **44** (2023), 106180. https://doi.org/10.1016/j.rinp.2022.106180

11. M. A. Abdou, A generalized auxiliary equation method and its applications, *Nonlinear Dyn.*, **52** (2008), 95–102. https://doi.org/10.1007/s11071-007-9261-y

12. G. L. Lamb Jr., Bäcklund transformations for certain nonlinear evolution equations, *J. Math. Phys.*, **15** (1974), 2157–2165. https://doi.org/10.1063/1.1666595

13. J.-H. He, X.-H. Wu, Exp-function method for nonlinear wave equations, *Chaos Soliton. Fract.*, **30** (2006), 700–708. https://doi.org/10.1016/j.chaos.2006.03.020

14. S. A. El-Wakil, M. A. Abdou, The extended Fan sub-equation method and its applications for a class of nonlinear evolution equations, *Chaos Soliton. Fract.*, **36** (2008), 343–353. https://doi.org/10.1016/j.chaos.2006.06.065

15. J.-H. He, Homotopy perturbation method: a new nonlinear analytical technique, *Appl. Math. Comput.*, **135** (2003), 73–79. https://doi.org/10.1016/S0096-3003(01)00312-5

16. M. S. Islam, K. Khan, A. H. Arnous, Generalized Kudryashov method for solving some (3+1)-dimensional nonlinear evolution equations, *New Trends in Mathematical Sciences*, **3** (2015), 46–57.

17. J. Hietarinta, Introduction to the Hirota bilinear method, In: *Integrability of nonlinear systems*, Berlin, Heidelberg: Springer, 1997, 95–103. https://doi.org/10.1007/BFb0113694

18. Y. Gurefe, E. Misirli, A. Sonmezoglu, M. Ekici, Extended trial equation method to generalized nonlinear partial differential equations, *Appl. Math. Comput.*, **219** (2013), 5253–5260. https://doi.org/10.1016/j.amc.2012.11.046

19. C. Gu, H. Hu, Z. Zhou, *Darboux transformations in integrable systems: theory and their applications to geometry*, Dordrecht: Springer, 2005. https://doi.org/10.1007/1-4020-3088-6

20. N. A. Kudryashov, Method for finding highly dispersive optical solitons of nonlinear differential equations, *Optik*, **206** (2020), 163550. https://doi.org/10.1016/j.ijleo.2019.163550

21. J. Zhang, X. Wei, Y. Lu, A generalized G'/G-expansion method and its applications, *Phys. Lett. A*, **372** (2008), 3653–3658. https://doi.org/10.1016/j.physleta.2008.02.027

22. S. M. Mirhosseini-Alizamini, H. Rezazadeh, M. Eslami, M. Mirzazadeh, A. Korkmaz, New extended direct algebraic method for the Tzitzica type evolution equations arising in nonlinear optics, *Comput. Methods Differ.*, **8** (2020), 28–53. https://doi.org/10.22034/CMDE.2019.9472

23. M. A. E. Abdelrahman, E. H. M. Zahran, M. M. A. Khater, The $\exp(-\phi(\Xi))$-expansion method and its application for solving nonlinear evolution equations, *International Journal of Modern Nonlinear Theory and Application*, **4** (2015), 37–47. https://doi.org/10.4236/ijmnta.2015.41004

24. S. A. El-Wakil, M. A. Abdou, The extended mapping method and its applications for nonlinear evolution equations, *Phys. Lett. A*, **358** (2006), 275–282. https://doi.org/10.1016/j.physleta.2006.05.040

25. E. Hussain, Z. Li, S. A. A. Shah, E. A. Az-Zo'bi, M. Hussien, Dynamics study of stability analysis, sensitivity insights and precise soliton solutions of the nonlinear (STO)-Burger equation, *Opt. Quant. Electron.*, **55** (2023), 1274. https://doi.org/10.1007/s11082-023-05588-w

26. Z. Li, E. Hussain, Qualitative analysis and optical solitons for the (1+1)-dimensional Biswas–Milovic equation with parabolic law and nonlocal nonlinearity, *Results Phys.*, **56** (2024), 107304. https://doi.org/10.1016/j.rinp.2023.107304

27. S. A. A. Shah, E. Hussain, W.-X. Ma, Z. Li, A. E. Ragab, T. M. Khalaf, Qualitative analysis and new variety of soliton profiles for the (1+1)-dimensional modified equal-width equation, *Chaos Soliton. Fract.*, **187** (2024), 115353. https://doi.org/10.1016/j.chaos.2024.115353

28. S. Malik, S. Kumar, A. Das, A (2+1)-dimensional combined KdV-mKdV equation: integrability, stability analysis and soliton solutions, *Nonlinear Dyn.*, **107** (2022), 2689–2701. https://doi.org/10.1007/s11071-021-07075-x

29. A. Zabihi, M. T. Shaayesteh, H. Rezazadeh, R. Ansari, N. Raza, A. Bekir, Solitons solutions to the high-order dispersive cubic–quintic Schrödinger equation in optical fibers, *J. Nonlinear Opt. Phys.*, **32** (2023), 2350027. https://doi.org/10.1142/S0218863523500273

30. Md. T. Islam, Md. A. Akbar, J. F. Gómez-Aguilar, E. Bonyah, G. Fernandez-Anaya, Assorted soliton structures of solutions for fractional nonlinear Schrödinger-type evolution equations, *J. Ocean Eng. Sci.*, **7** (2022), 528–535. https://doi.org/10.1016/j.joes.2021.10.006

31. Beenish, E. Hussain, U. Younas, R. Tapdigoglu, M. Garayev, Exploring bifurcation, quasi-periodic patterns, and wave dynamics in an extended Calogero-Bogoyavlenskii-Schiff model with sensitivity analysis, *Int. J. Theor. Phys.*, **64** (2025), 146. https://doi.org/10.1007/s10773-025-06008-3

32. K.-J. Wang, Variational principle and diverse wave structures of the modified Benjamin-Bona-Mahony equation arising in the optical illusions field, *Axioms*, **11** (2022), 445. https://doi.org/10.3390/axioms11090445

33. S. Singh, S. S. Ray, Integrability and new periodic, kink-antikink and complex optical soliton solutions of (3+1)-dimensional variable coefficient DJKM equation for the propagation of nonlinear dispersive waves in inhomogeneous media, *Chaos Soliton. Fract.*, **168** (2023), 113184. https://doi.org/10.1016/j.chaos.2023.113184

34. E. H. Zahran, S. M. Mirhosseini-Alizamini, M. S. M. Shehata, H. Rezazadeh, H. Ahmad, Study on abundant explicit wave solutions of the thin-film Ferro-electric materials equation, *Opt. Quant. Electron.*, **54** (2022), 48. https://doi.org/10.1007/s11082-021-03296-x

35. X. Pu, W. Zhou, The hydrostatic approximation of the Boussinesq equations with rotation in a thin domain, *Nonlinear Anal.*, **251** (2025), 113688. https://doi.org/10.1016/j.na.2024.113688

36. I. Ul. Haq, N. Ali, S. Ahmad, T. Akram, A hybrid interpolation method for fractional PDEs and its applications to fractional diffusion and Buckmaster equations, *Math. Probl. Eng.*, **2022** (2022), 2517602. https://doi.org/10.1155/2022/2517602

37. W. A. Faridi, S. A. AlQahtani, The explicit power series solution formation and computation of Lie point infinitesimal generators: Lie symmetry approach, *Phys. Scripta*, **98** (2023), 125249. https://doi.org/10.1088/1402-4896/ad0948

38. Md. T. Islam, T. R. Sarkar, F. A. Abdullah, J. F. Gómez-Aguilar, Characteristics of dynamic waves in incompressible fluid regarding nonlinear Boiti-Leon-Manna-Pempinelli model, *Phys. Scripta*, **98** (2023), 085230. https://doi.org/10.1088/1402-4896/ace743

39. H. Zheng, Y. Xia, Persistence of solitary-wave solutions for the delayed regularized long wave equation under Kuramoto–Sivashinsky perturbation and Marangoni effect, *Chaos Soliton. Fract.*, **184** (2024), 115049. https://doi.org/10.1016/j.chaos.2024.115049

40. H. Zheng, Y. Xia, Bifurcation of the travelling-wave solutions in a perturbed (1+1)-dimensional dispersive long wave equation via a geometric approach, *Proc. Roy. Soc. Edinb. A*, in press. https://doi.org/10.1017/prm.2024.45

41. A.-M. Wazwaz, S. A. El-Tantawy, A new integrable (3+1)-dimensional KdV-like model with its multiple-soliton solutions, *Nonlinear Dyn.*, **83** (2016), 1529–1534. https://doi.org/10.1007/s11071-015-2427-0

42. I. M. Krichever, S. P. Novikov, Holomorphic bundles over algebraic curves and non-linear equations, *Russ. Math. Surv.*, **35** (1980), 53–79. https://doi.org/10.1070/RM1980v035n06ABEH001974

43. J. Weiss, M. Tabor, G. Carnevale, The Painlevé property for partial differential equations, *J. Math. Phys.*, **24** (1983), 522–526. https://doi.org/10.1063/1.525721

44. J. Weiss, The Painlevé property and Bäcklund transformations for the sequence of Boussinesq equations, *J. Math. Phys.*, **26** (1985), 258–269. https://doi.org/10.1063/1.526655

45. K. Toda, S.-J. Yu, The investigation into the Schwarz–Korteweg–de Vries equation and the Schwarz derivative in (2+1) dimensions, *J. Math. Phys.*, **41** (2000), 4747–4751. https://doi.org/10.1063/1.533374

46. J. Ramírez, J. L. Romero, M. S. Bruzón, M. L. Gandarias, Multiple solutions for the Schwarzian Korteweg–de Vries equation in (2+1) dimensions, *Chaos Soliton. Fract.*, **32** (2007), 682–693. https://doi.org/10.1016/j.chaos.2005.11.019

47. A. Nakamura, The Miura transform and the existence of an infinite number of conservation laws of the cylindrical KdV equation, *Phys. Lett. A*, **82** (1981), 111–112. https://doi.org/10.1016/0375-9601(81)90924-5

48. J. Mas, E. Ramos, The constrained KP hierarchy and the generalised Miura transformation, *Phys. Lett. B*, **351** (1995), 194–199. https://doi.org/10.1016/0370-2693(95)00357-Q

49. M. S. Velan, M. Lakshmanan, Lie symmetries, Kac-Moody-Virasoro algebras and integrability of certain (2+1)-dimensional nonlinear evolution equations, *J. Nonlinear Math. Phys.*, **5** (1998), 190–211. https://doi.org/10.2991/jnmp.1998.5.2.10

50. A. R. Seadawy, M. Iqbal, D. Lu, Applications of propagation of long-wave with dissipation and dispersion in nonlinear media via solitary wave solutions of generalized Kadomtsev–Petviashvili modified equal-width dynamical equation, *Comput. Math. Appl.*, **78** (2019), 3620–3632. https://doi.org/10.1016/j.camwa.2019.06.013

51. J. Wang, K. Shehzad, A. R. Seadawy, M. Arshad, F. Asmat, Dynamic study of multi-peak solitons and other wave solutions of new coupled KdV and coupled Zakharov–Kuznetsov systems with their stability, *J. Taibah Univ. Sci.*, **17** (2023), 2163872. https://doi.org/10.1080/16583655.2022.2163872

52. X. Li, M. Zhang, Darboux transformation and soliton solutions of the (2+1)-dimensional Schwarz–Korteweg–de Vries equation, *Mod. Phys. Lett. B*, **34** (2020), 2050270. https://doi.org/10.1142/S021798492050270X

53. Z. Li, Diversity soliton excitations for the (2+1)-dimensional Schwarzian KdV equation, *Therm. Sci.*, **22** (2018), 1781–1786. https://doi.org/10.2298/TSCI1804781L

54. M. A. S. Murad, M. A. Mustafa, Nonlinear conformable Schrödinger equation in weakly nonlocal media using a new generalized computational technique, *International Journal of Computational Mathematics*, in press. https://doi.org/10.1080/00207160.2025.2507677

55. M. L. Gandarias, M. S. Bruzón, J. Ramirez, Classical symmetry reductions of the Schwarz–Korteweg–de Vries equation in 2+1 dimensions, *Theor. Math. Phys.*, **134** (2003), 62–71. https://doi.org/10.1023/A:1021867622943

56. M. A. S. Murad, S. S. Mahmood, H. Emadifar, W. W. Mohammed, K. K. Ahmed, Optical soliton solution for dual-mode time-fractional nonlinear Schrödinger equation by generalized exponential rational function method, *Results Eng.*, **27** (2025), 105591. https://doi.org/10.1016/j.rineng.2025.105591

AIMS Press